Proceedings of 2004 IEEE/RSJ International Conference on Intelligent Robots and Systems
September 28 - October 2, 2004, Sendai, Japan

Fast Shape-based Road Sign Detection for a Driver Assistance System

Gareth Loy
Computer Vision and
Active Perception Laboratory
Royal Institute of Technology (KTH)
Stockholm, Sweden
Email: gareth@nada.kth.se

Nick Barnes
Autonomous Systems and
Sensor Technologies Program
National ICT Australia
Canberra, Australia
Email: nick.barnes@nicta.com.au

Abstract—**A new method is presented for detecting triangular, square and octagonal road signs efficiently and robustly. The method uses the symmetric nature of these shapes, together with the pattern of edge orientations exhibited by equiangular polygons with a known number of sides, to establish possible shape centroid locations in the image. This approach is invariant to in-plane rotation and returns the location and size of the shape detected. Results on still images show a detection rate of over 95%. The method is efficient enough for real-time applications, such as on-board-vehicle sign detection.**

I. Introduction

Improving safety is a key goal in road vehicle development. Driver support systems that help drivers react to changing road conditions can potentially improve safety. Our research focusses on systems that support the driver in controlling the car, whilst keeping the driver in the loop.

Sign recognition is an important task for a driver support system. Signs give useful information and appear clearly in the environment. However, drivers sometimes miss signs due to distractions or lack of concentration. It may then be helpful to make them aware of the information they have missed. Two approaches are useful here for different types of sign: critical signs and information signs. For critical signs, the driver should make an adjustment in their control of the vehicle. An in-car system can perceive whether the driver is already aware of a critical sign by his or her reaction or lack of it, e.g. not slowing down in response to speed signs, or failing to react to stop or give way signs. For less urgent information signs, such as warning or direction signs, a recent sign could simply appear on a discrete display that the driver can view when convenient.

The fast radial symmetry operator [1] provides an efficient means for finding radially symmetric features in images. In particular, it has been shown to effectively detect the circles on Australian speed signs, reliably identifying potential speed sign locations in images from a vehicle based vision platform [2]. We generalise this method to detect triangular, diamond (square) and octagonal signs, generating detectors fast enough to run at many frames per second.

We present an algorithm to detect the class of shapes containing regular polygons and circles. These can be viewed as circles represented by a number of equilateral .and equiangular linear edges, where the number of edges varies between three (a triangle) to infinite (a circle). This class encapsulates most of the common sign types, i.e., triangular, diamond, square, octagonal, and round. Our algorithm detects these shapes robustly and quickly.

This class of detectors has complexity $\mathcal{O}(Nkl)$, where l is the maximum length of the segments, k is the number of radii (scales) being considered, and N is the number of pixels in the image. Note that for small shapes, l and k are small numbers. Comparable algorithms such as the generalised Hough transform [3] are far more computationally complex. Even recent high speed implementations of the generalised Hough transform on specialised hardware take multiple seconds to recognise a single shape [4].

Other general work on perceptual grouping [5] takes a similar approach in terms of finding local support for shapes. However, this work does not use pixel-based gradient information, and works at the level of edge segments for gradient. A complexity of k^2 was reported where k is the number of edge segments, however, for a cluttered image, if the segment size is one pixel, k may be of the order of the size of the image.

The class of shape detectors presented in this paper is specialised for real-time performance by exploiting the nature of shapes that vote to a centre point. This makes the algorithm robust to missing pixels due to lack of contrast or incorrect gradient direction estimates, as the vote for the centre-point will be high. These shape detectors are parametric in their formulation, and can be applied easily and efficiently in situations where constraints are available from the embodiment of the vision system, such as the appearance of road signs to a car. This is in keeping with the embodied vision algorithm approach [6], exploiting the constraints of the system the algorithm is placed within to facilitate fast and robust computation.

Our shape detection approach has strong robustness to changing illumination as it detects shapes based on edges, and will efficiently reduce the search for a road sign from the whole image to a small number of pixels. The real advantages become apparent when our detectors are considered as part of a system with a sign recognition technique. With traditional detection methods that return regions of interest, every pixel in these regions must be

0-7803-8463-6/04/$20.00 ©2004 IEEE

searched, for every size of sign that can appear, as well as every possible sign. However, our new detectors accurately return the centroid, scale and shape of candidate signs. Thus, few pixels need to be examined for recognition and the shape and size are known. Subsequent computation is well targeted, and comparatively little computation is needed to assess a candidate.

II. Background

Road sign recognition research has been around since the mid 1980's. A direct approach is to apply normalised cross-correlation to the raw traffic scene image. This is computationally prohibitive, but can be eased somewhat by approaches such as simulated annealing [7]. Another method for controlling computation is presented by [8]: applying templates to an edge image of the road scene. A distance-to-nearest-feature transform is applied to smooth the matching space for coarse-to-fine matching, and a hierarchical structure of templates eases the burden of a large number of templates. However, this is still computationally intensive and so unsuitable for an in-the-loop system.

Many approaches have used separate stages for sign detection and classification of different types of sign [9], [10], [11], [12]. Especially when a large number of sign types are to be classified. We argue this can be an effective means of managing computation for even a small number of sign types if detection can be efficiently achieved. Further, this can facilitate real-time operation by allowing possibly computationally intensive classification to be performed on only a small part of the image, without requiring assumptions about where signs may appear.

Colour segmentation is the most common method for the initial detection of signs. Typically, this is based on the assumption that the wavelength arriving at the camera from a traffic sign is invariant to the intensity of incident light. This assumption usually manifests in the statement that HSV (or HSI) space is invariant to lighting conditions [12]. A great deal of the research in this area exploits a detection stage based on this assumption [12], [13], [9], [11], [14], [15], [16], either finding the signs, or eliminating much of the image from further processing. However, the camera image is *not* invariant to changes in the chromaticity of the incident light. Further, as signs fade over time the colour of the signs is not invariant.

Another approach to detection is *a priori* assumptions about image formation. For instance, assuming the road is approximately straight allows large portions of the image to be ignored when looking for signs. Combined with colour segmentation, Hsu and Huang [16] look for signs in only a restricted part of the image. However, such assumptions can break down on curved roads, or with bumps such as speed humps. A more sophisticated approach is to use some form of detection to facilitate scene understanding, and thus eliminate a large region of the image. For example, Piccoli *et. al* [13] suggest large uniform regions of the image correspond to road and sky, and thus only look alongside the road and below the sky where signs are likely to appear. However, this is inadequate in cluttered road scenes, such as tree-lined streets. They also suggest ignoring one side of the image as relevant signs will only appear on one side. This is not the case, however, on dual carriageways where signs typically appear on both sides of the road.

In this paper we present an application of a new class of shape detectors to visual road sign detection. Our approach uses gradient elements to detect signs based on shape. Triangular, square, diamond, octagonal and circular signs can be detected in this manner.

III. Road Environment Structure

There is much possible variation in the appearance of a sign in an image. Throughout the day, and at night time, lighting conditions can vary enormously. A sign may be well lit by direct sunlight, or headlights, it may be completely in shadow on a bright day, or heavy rain may blur the image of the sign. Ideally, signs have clear colour contrast, but over time they can become faded, yet still be clear to drivers. Although signs appear by the road edge, this may be far from the car on a multi-lane highway – to the left or right, or very close on a single lane exit ramp. Further, while signs are generally a standard distance above the ground, they can also appear on temporary roadwork signs at ground level. Thus it is not simple to restrict the possible positions of a sign within an image of a road scene. By modelling the road [17], it may be possible to dictate parts of the image where a sign cannot appear, but road modelling has its own computational expense, and, as discussed previously, colour-based methods are not robust.

However, the roadway is well structured, and the appearance of road signs is highly restricted. They must be of a particular size, and have particular colours and shapes for individual signs. Unless the sign has been tampered with, signs will appear approximately orthogonally to the road direction. Finally, signs are always placed, so the driver can easily see them without having to look away from the road. Typically, we can assume signs are upright alongside the road, however, with minor accidents, signs can occasionally appear tilted, our detectors are robust to this variation.

Our algorithm searches the image for features of the expected shapes. As signs almost always appear in the orthogonal direction to the road, provided our camera points in the direction of vehicle motion, the surface of all signs will be parallel to the image plane of the camera. On a rapidly curving road it may be that the sign only appears parallel to the image plane briefly, but this will be when the vehicle is close to the sign, so it will appear large in the image. If we are processing images at frame rate, and we are able to recognise a sign reliably from only a small number of frames then generally we are safe to assume that the sign is parallel to the image plane.

IV. Detecting Road Sign Candidates

A. Shape Detection Method

We extend the fast radial symmetry transform [1] to detect regular polygons. This method operates on the gradient of a gray-scale image. Firstly, insignificant gradient elements, whose magnitudes are less than a specified

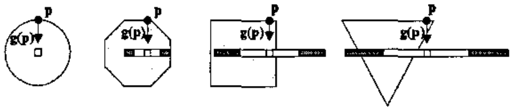

Fig. 1. Voting lines associated with a gradient element when searching for different shapes.

threshold[1], are set to zero and the remaining elements normalised. Each remaining non-zero gradient element votes for a potential circle centre a distance r away (where r is the radius of the circle being targeted) along the line of the gradient vector. The vote is placed at the closest pixel to this point.

The points voted for are called *affected pixels* and are defined by:

$$\mathbf{p}_{\pm ve}(\mathbf{p}) = \mathbf{p} \pm \text{round}\left(r\mathbf{g}(\mathbf{p})\right),$$

where $\mathbf{g}(\mathbf{p})$ is the unit gradient at point $\mathbf{p}$. There are positive $\mathbf{p}_{+ve}$ and negative $\mathbf{p}_{-ve}$ affected pixels corresponding to points that the gradient points towards and away from respectively. Since we do not know *a priori* whether a sign will be lighter or darker than the background we use both positively and negatively affected pixels concurrently. However, if such information is known it can be used.

To extend this voting scheme to regular polygons we define the 'radius' of a polygon as the perpendicular distance from an edge to the centroid. Further, rather than gradient elements voting for a single point, a line of votes is cast describing possible shape centroid positions that would account for the observed gradient element.

Figure 1 shows different votes cast by a gradient element $\mathbf{g}(\mathbf{p})$ when searching for different shapes at a given radius (only the votes associated with the positively affected pixel are shown). Whereas in the case of a circle a single vote is cast per gradient element, a line of votes is cast when searching for straight-sided shapes. The white bars indicate potential centroid locations that receive a positive vote, and the dark bars indicate locations that receive a negative vote. The negative voting is introduced to attenuate the response generated by straight lines too long to correspond to shape edges at the target radius.

The length of the line of pixels voted for is defined by w as shown in Figure 2. The width parameter w is chosen so that every point on a shape edge will cast a vote for the correct shape centroid, and is given by:

$$w = \text{round}\left(r \tan\frac{\pi}{n}\right),$$

where r is the radius and n the number of sides of the polygon being targeted.

The line on which the affected pixels lie can be approximated by:

$$L(\mathbf{p},\mathbf{m}) = \mathbf{p}_{\pm \mathbf{ve}}(\mathbf{p}) + \text{round}\left(m\bar{\mathbf{g}}(\mathbf{p})\right),$$

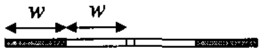

Fig. 2. Line of pixels voted for by a gradient element

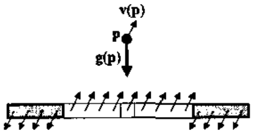

Fig. 3. Example of n-angle gradient projected from a point $\mathbf{p}$

where $\bar{\mathbf{g}}(\mathbf{p})$ is a unit vector perpendicular to $\mathbf{g}(\mathbf{p})$. The pixels receiving a positive vote are then given by:

$$L(\mathbf{p},\mathbf{m})|m \in [-w, w],$$

and those receiving a negative vote by:

$$L(\mathbf{p},\mathbf{m})|m \in [-2w, -w-1] \cup [w+1, 2w].$$

Whether targeting circles or regular polygons, all votes are accumulated into a vote image $\mathbf{O}_r$. Figure 4 (b) shows an example vote image for an octagonal target.

Regular polygons are equiangular i.e., their sides are separated by a regular angular spacing; for an n-sided polygon this is $360/n$ degrees. To improve our detection of these shapes we introduce a rotationally invariant measure of how well a set of edges fits a particular angular spacing.

Define $\gamma(x,y) = n\theta(x,y)$ where $\theta = \angle\mathbf{g}$ is the gradient angle, and n is the number of sides of the target polygon. Let $\mathbf{v}$ be the unit vector field such that $\angle\mathbf{v}(x,y) = \gamma(x,y)$. For a given set of edge points $\mathbf{p}_i$, the magnitude of the vector sum $\sum_i \mathbf{v}(\mathbf{p}_i)$ indicates how well the set of edges $\mathbf{g}(\mathbf{p}_i)$ fits the angular spacing defined by n.

Consider the example in Figure 5. Three edge points $\mathbf{p}_i$ are sampled from the sides of an equilateral triangle. The unit gradient vectors and their associated angles are shown in (a). By multiplying the gradient angles by n ($n = 3$ for a triangle) the resulting vectors share the same direction if, and only if, their original orientations were spaced $360/n$ degrees apart. Thus the magnitude of the vector sum of these n-angle vectors is maximal if the edge points occur at the targeted angular spacing.

To utilise this result we construct a vector field of projected n-angle gradients by considering each non-zero element of $\mathbf{g}$ and projecting its associated n-angle vector $\mathbf{v}(\mathbf{p})$ onto its voting space as shown in Figure 3 (note the sign is reversed when projecting onto negatively voted pixels). Vectors projected onto the same pixel are summed. The result is a vector field $\mathbf{B}_r$, whose magnitude indicates how well the gradient elements voting on each point match the target angular spacing. Figure 4 (c) shows an example of such a magnitude image for an octagonal target.

For increasing n the n-angle representation is limited by the accuracy of the gradient orientation estimate. However, it is perfectly adequate for $n = 8$ (e.g. Figure 4 (c)) which is the maximum required for road sign detection.

[1] A threshold equal to 5% of the maximum possible gradient magnitude was used for our experiments.

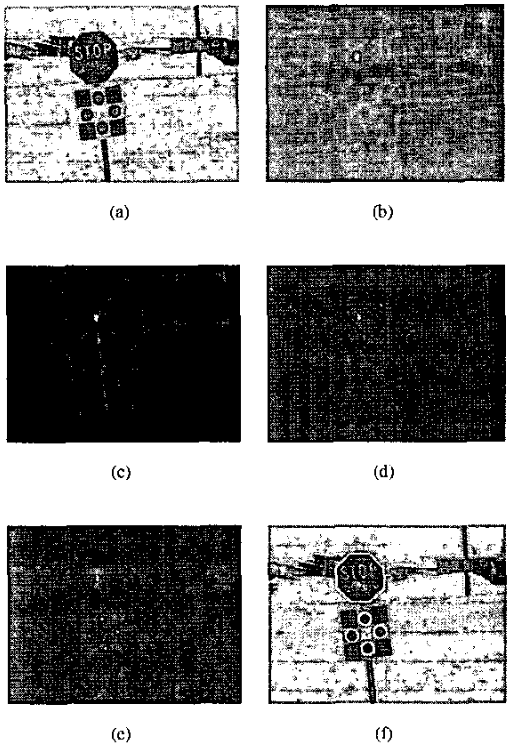

Fig. 4. Searching for octagons in an image. (a) original 300 × 400 image, (b) vote image $\mathbf{O}_r$ for $r = 40$ (c) magnitude of equiangular image $||\mathbf{B}_r||$ for $r = 40$ (d) result for radius $r = 40$, (e) total result over all radii $r \in [6, 40]$, (f) detected octagons.

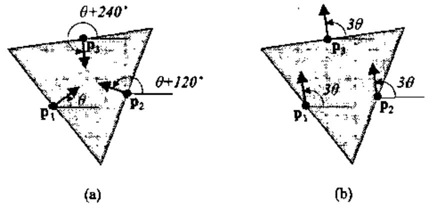

Fig. 5. Example of three edge points $\mathbf{p}_i$ on a triangle. Showing (a) the angles of the unit gradient vectors, and (b) the resulting vectors obtained by multiplying the gradient angles by n ($n = 3$)

```
1) Determine the gradient vector field. Threshold the magnitude, setting values below the threshold to zero and those above to unity. Denote the output $\mathbf{g}$.
2) Determine the $n$-angle gradient such that $||\mathbf{v}|| = ||\mathbf{g}||$ and $\angle\mathbf{v} = n\angle\mathbf{g}$.
3) For each radius under consideration:
    a) Consider each non-zero element of $\mathbf{g}$ in turn, for each such element:
        i) Determine the vote locations.
        ii) Accumulate the contribution to the vote image $\mathbf{O}_r$, and the equiangular image $\mathbf{B}_r$.
    b) Calculate the output image $\mathbf{S}_r$ at radius $r$, as $\mathbf{O}_r(\mathbf{p})\mathbf{B}_r(\mathbf{p})$, and accommodate for scale.
4) Sum $\mathbf{S}_r$ over all radii $r \in R$ to determine the final output image $\mathbf{S}$.
```

Fig. 6. Summary of the algorithm.

Once the vote image $\mathbf{O}_r$ and the equiangular image $\mathbf{B}_r$ have been computed the final shape response $\mathbf{S}_r$ is determined for the radius in question as:

$$\mathbf{S}_r(\mathbf{p}) = \frac{\mathbf{O}_r(\mathbf{p})||\mathbf{B}_r(\mathbf{p})||}{(2wr)^2}.$$

The denominator is a scaling factor that facilitates comparisons of results across different radii.

The n-angle representation is not relevant to circles since a circle has edges at all orientations, however, in principle $||\mathbf{B}_r||$ can still be computed by summing relevantly orientated (all) vectors voting on each point, giving $||\mathbf{B}_r|| = \mathbf{O}_r$, which makes the circular radial symmetry algorithm [1] an extrema in this class of algorithms.

The transform is typically calculated over a set of radii $r \in R$, where R is the set of radii values at which the road sign is expected to appear. The combined result image $\mathbf{S}$ is obtained by summing over all $r \in R$.

When searching across multiple radii, maxima are first identified in the combined image $\mathbf{S}$, then verified to appear with sufficient magnitude in one or more of the radial results $\mathbf{S}_r$ from which the position and radius are determined.

Figure 6 presents an overview of the algorithm, and Figure 4 shows outputs at different stages of the detection of octagons in an example image. Note that although the size and location of the shapes are recovered the orientation is not since the operator is orientation invariant (the detected octagons are drawn with zero orientation).

B. Implementation and real-time issues

To adapt the algorithm for road sign detection, it need only be applied to radii practical for detecting signs in traffic images. A shape with a small number of pixels as its radius may well constitute a sign, however, there will be insufficient pixels present to discern what the sign says, and so there is no point in further processing until the sign is close enough to be recognised. Also in normal driving conditions a sign will never appear closer to the camera than several metres. Given a camera of approximately known focal length, we can impose an upper limit on the possible radius of shapes to look for. As the basic shape of a sign will be clear, even if it is faded, we set a threshold that requires a large number of the possible edge pixels to be detected. Further consistency checking can be performed over time i.e., a shape must appear for at least two concurrent frames, its radius must not have changed greatly during that time, and it must not move far in the image.

Previously [2] we demonstrated that shape detection can combine effectively with classification. With the circle detector only, the fast radial symmetry detector, 40 and 60 signs were detected and classified correctly in the vast majority of cases using normalised cross-correlation.

This was based on a bank of sign templates covering the expected radii. The candidate radius was identified by the detector, only that template and the ones nearest to it were correlated over a 5×5 region around the extracted centroid of the sign. The full classification was implemented in C++ to evaluate real-time performance. For a 320×240 image, the full radial symmetry detection and classification was able to be run at 20Hz, with classification taking $\leq$ 1ms. Figure 7 (b) shows an example of a detected and correctly classified frame taken during the operation of this system.

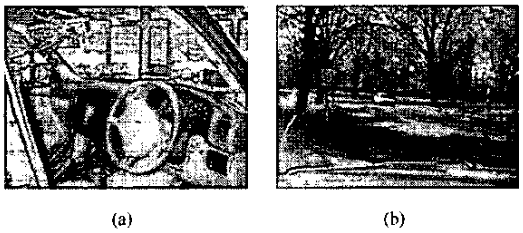

Fig. 7. (a) The ANU/NICTA Intelligent Vehicle. The cameras are mounted where the rear view mirror would be. (b) Speed sign detection and classification system in operation.

V. Performance

Performance was tested on a diverse set of 45 images containing road signs. A large collection of such images was obtained via Google, from which test images were randomly selected and sub-sampled to a common size. Each shape detector was tested on 15 images containing road signs of the targeted shape, Figure 8 shows a representative sample of these images annotated with the detection results generated by the algorithm.

The results are summarised in Table I and show strong detection performance across all shapes. The algorithm only fails in two instances and these are shown in Figure 10. In one case this is due to occlusion (a), whilst the other (b) is caused by lack of contrast and indistinct edge between the sign and the background. The occlusion would not occur if the stop sign was viewed from the road – generally roads are maintained to ensure such signs are not occluded. The case of failure due to insufficient contrast can be addressed by taking gradients on all colour channels and summing the results (in these results only gray-scale gradients were used). The yellow sign in Figure 10 (b) stands out as a dark diamond in the blue colour channel.

Figure 9 shows some of the more challenging signs detected by the algorithm. These include unorthodox octagonal signs in (a) and (b) that would not be detected by a colour-based scheme looking for red stop signs; (c) a triangular sign viewed from a non-fronto-parallel perspective and partly obscured by foliage; and (d) a diamond sign against a cluttered background providing little contrast with the sign.

The lack of false positives for the octagonal signs can be attributed to their distinctive shape and angular spacing – there are few other 'octagon-like' shapes likely to occur in an image. The square, diamond and triangle shapes, however, occur more prevalently and whilst the majority of the shapes detected did correspond to instances of these shapes, these did not always correspond to road signs. Nonetheless, this is not a problem for our algorithm, since its purpose is to efficiently find *potential* sign locations. Furthermore, when applying this method to video taken onboard a vehicle temporal consistency can be used to discard many accidental views that do not correspond to approaching signs (as per [2]).

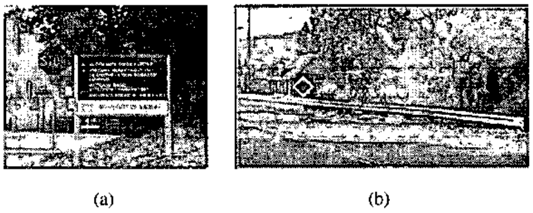

Fig. 10. Instances where sign detection failed

TABLE I

PERFORMANCE ON STILL IMAGES

Shape	Correctly detected	No. false positives	No. targets
octagon	95%	0	15
square	95%	15	19
triangle	100%	10	15

VI. Conclusion

A novel shape-based technique was introduced and applied to detecting road signs in images. The method extends the concept of the fast radial symmetry transform to detect regular polygons. It was tested on a range of images containing road signs and correctly detected signs in over 95% of cases. The method is invariant to in-plane rotation, being able to detect signs viewed at any orientation, and returns the location and size of the shape detected. The low complexity of the algorithm makes it suited for real-time sign detection onboard an intelligent vehicle.

Acknowledgments

The support of the STINT foundation through the KTH-ANU grant IG2001-2011-03 is gratefully acknowledged.

National ICT Australia is funded by the Australian Department of Communications, Information Technology and the Arts and the Australian Research Council through *Backing Australia's ability* and the ICT Centre of Excellence Program.

References

[1] G. Loy and A. Zelinsky, "Fast radial symmetry for detecting points of interest," *IEEE Trans Pattern Analysis and Machine Intelligence*, vol. 25, no. 8, pp. 959–973, Aug. 2003.

[2] N. Barnes and A. Zelinsky, "Real-time radial symmetry for speed sign detection," in *Proc IEEE Intelligent Vehicles Symposium*, Parma, Italy, 2004.

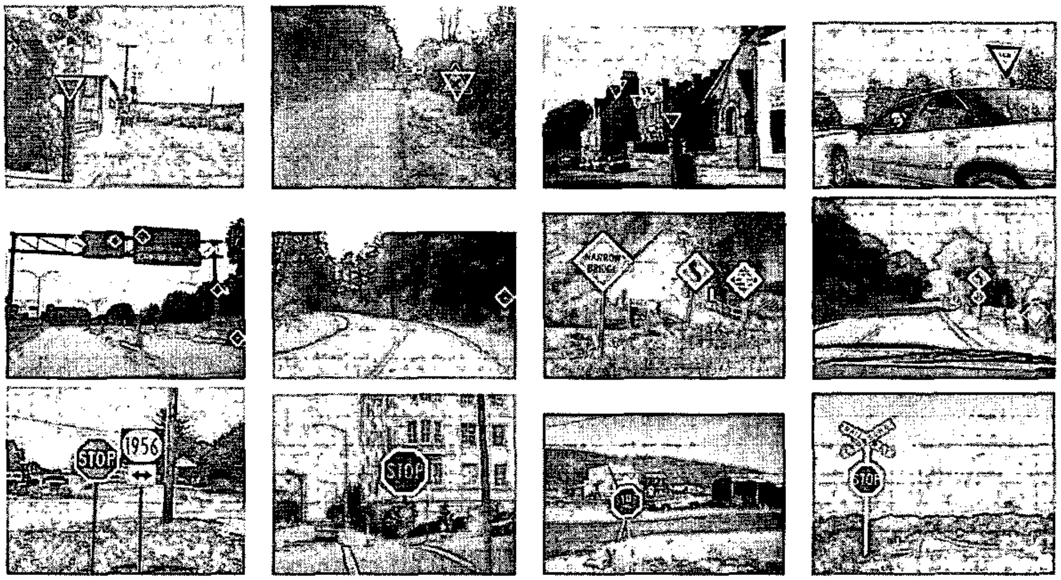

Fig. 8. Results for searching for triangles (top row) with $r \in \{8, 10, .., 18\}$, and squares (middle row) and octagons (bottom row) with $r \in \{10, 12, 14, 17, 20, 25\}$. All targeted signs are correctly detected.

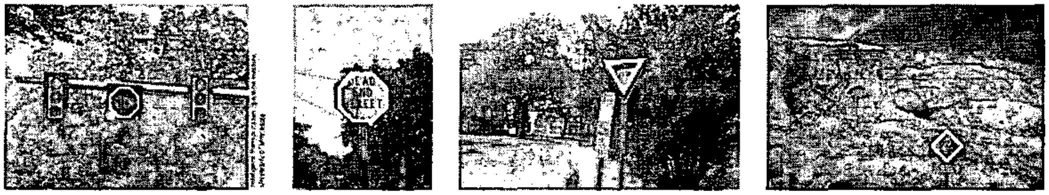

(a) (b) (c) (d)

Fig. 9. Difficult tests

[3] D. H. Ballard, "Generalizing the hough transform to detect arbitrary shapes," *Pattern Recognition*, vol. 13, no. 2, pp. 111–122, 1981.

[4] R. Strzodka, I. Ihrke, and M. Magnor, "A graphics hardware implementation of the generalized hough transform for fast object recognition, scale and 3d pose detection," in *Proc 12th Int Conf on Image Analysis and Processing*, Mantova, Italy, 2003, pp. 188–193.

[5] G. Guy and G. Medioni, "Inferring global perceptual contours from local features," *International Journal of Computer Vision*, vol. 20, no. 1-2, pp. 113–333, Oct. 1996.

[6] N. M. Barnes and Z. Q. Liu, "Embodied categorisation for vision-guided mobile robots," *Pattern Recognition*, vol. 37, no. 2, pp. 299–312, Feb. 2004.

[7] M. Betke and N. Makris, "Fast object recognition in noisy images using simulated annealing," A.I. Lab, M.I.T., Cambridge, Mass, USA, Tech. Rep. AIM-1510, 1994.

[8] D. M. Gavrila, "A road sign recognition system based on dynamic visual model," in *Proc 14th Int. Conf. on Pattern Recognition*, vol. 1, Aug 1998, pp. 16–20.

[9] P. Paclik, J. Novovicova, P. Somol, and P. Pudil, "Road sign classification using the laplace kernel classifier," *Pattern Recognition Letters*, vol. 21, pp. 1165–1173, 2000.

[10] J. Miura, T. Kanda, and Y. Shirai, "An active vision system for real-time traffic sign recognition," in *Proc 2000 IEEE Int Vehicles Symposium*, Oct 2002, pp. 52–57.

[11] B. Johansson, "Road sign recognition from a moving vehicle," Master's thesis, Centre for Image Analysis, Swedish University of Agricultural Sciences, 2002.

[12] L. Priese, J. Klieber, R. Lakmann, V. Rehrmann, and R. Schian, "New results on traffic sign recognition," in *Proceedings of the Intelligent Vehicles Symposium*. Paris: IEEE Press, Aug. 1994, pp. 249–254. [Online]. Available: citeseer.nj.nec.com/priese94new.html

[13] G. Piccioli, E. D. Micheli, P. Parodi, and M. Campani, "Robust method for road sign detection and recognition," *Image and Vision Computing*, vol. 14, no. 3, pp. 209–223, 1996.

[14] C. Y. Fang, C. S. Fuh, S. W. Chen, and P. S. Yen, "A road sign recognition system based on dynamic visual model," in *Proc IEEE Conf. on Computer Vision and Pattern Recognition*, vol. 1, 2003, pp. 750–755.

[15] D. G. Shaposhnikov, L. N. Podladchikova, A. V. Golovan, and N. A. Shevtsova, "A road sign recognition system based on dynamic visual model," in *Proc 15th Int Conf on Vision Interface*, Calgary, Canada, 2002.

[16] S.-H. Hsu and C.-L. Huang, "Road sign detection and recognition using matching pursuit method," *Image and Vision Computing*, vol. 19, pp. 119–129, 2001.

[17] R. Labayrade, D. Aubert, and J.-P. Tarel, "Real time obstacle detection in stereovision on non flat road geometry through v-disparity representation," in *Proc IEEE Int Vehicles Symposium*, June 2002.